

## RESEARCH ARTICLE

# Trends in return levels of 24-hr precipitation extremes during the typhoon season in Taiwan

Pao-Shin Chu<sup>1</sup>  | Hanpei Zhang<sup>1</sup> | Hui-Ling Chang<sup>2</sup> | Tsui-Ling Chen<sup>2</sup> | Kristine Tofte<sup>1</sup>

<sup>1</sup>Department of Atmospheric Sciences, School of Ocean and Earth Science and Technology, University of Hawaii-Manoa, Honolulu, Hawaii

<sup>2</sup>Research and Development Center, Central Weather Bureau, Taipei, Taiwan

**Correspondence**

Pao-Shin Chu, Department of Atmospheric Sciences, School of Ocean and Earth Science and Technology, University of Hawaii-Manoa, Honolulu, HI 96822.

Email: chu@hawaii.edu

**Funding information**

Central Weather Bureau (CWB) of the Republic of China

This study is to investigate changes in maximum 24-hr precipitation for 20 stations during the typhoon season (July–October) and how the El Niño–Southern Oscillation (ENSO) may modulate precipitation extremes in Taiwan. Based on the non-parametric Mann–Kendall method and Sens’s test, 15 out of 20 stations (three fourth) exhibited an upward trend from 1958 to 2013. Results of the field significance test suggest that the significant increasing trend is not caused by random variability.

The method of the non-stationary generalized extreme value distribution (NGEV) is then applied to determine temporal changes in return levels. Results show that a large majority of stations are marked by an increasing trend in the three chosen return levels (2, 20, and 100 years) over the last 56 years. Therefore, more intense typhoon producing seasonal maximum 24-hr precipitation has been observed in Taiwan. The waiting time for an extreme event to occur has shortened considerably in recent years. For stations located in western/central Taiwan, an El Niño (La Niña) event favours low (high) precipitation extremes. It is the opposite for stations in northern and eastern Taiwan. Thus, an east–west regional difference in precipitation extremes across Taiwan is noted. A NGEV model based on both time and ENSO as covariates is also applied. Inter-annual variations influenced by ENSO are more dominant than long-term trend in return levels for most stations in western/central Taiwan.

**KEYWORDS**

NGEV, return levels, precipitation extremes, Taiwan

## 1 | INTRODUCTION

Extreme climatic events, such as heavy precipitation and associated flooding, attract a lot of attention because of their potential damage to human societies and their adverse economic impacts. For instance, a heavy downpour in a short-time span can trigger landslides and mudflows in mountainous regions. This may result in property damage and loss of human and animal life, along with severe environmental degradation. Rainfall-frequency statistics are vital for a variety of hydro-meteorological and engineering designs, environmental regulations, risk analysis, and disaster prevention purposes. For instance, hydrologists need to know these statistics when designing storm drainage standards, in

determining streamflow peak discharges, and estimating flood potential within watersheds expected from rainstorms.

Specifically, it is necessary to know the amount of rainfall that can be expected to occur in a given time interval (e.g., 3 and 24 hr) for the average of a period of many years (e.g., 20 and 100 years). The average “return periods” are derived from quantiles of a particular probability distribution on the basis of extreme value theory. The generalized extreme value (GEV) distribution is often found to be a good approximation for the statistics of the maxima of long sequences of random variables (Coles, 2001; Wilks, 2011). The GEV distribution is characterized by three parameters—location, scale, and shape. The probability density function of GEV can be integrated analytically to yield the

cumulative distribution function (CDF), which can then be inverted to yield an explicit formula for the quantile function. This makes GEV very appealing because once the three distribution parameters are known, its extreme value (e.g., 358 mm within 24 hr) corresponding to any desired return period (e.g., 50 and 100 years) can be immediately determined. This extreme value is also known as the return level, which is expressed as the same unit as rainfall. The data set used for the GEV distribution is often the annual maximum daily rainfall. That is, the largest single 24-hr value in each of  $n$  years, known as the block maximum series, is chosen (Zwiers and Kharin, 1998; Kharin and Zwiers, 2005; Garcia *et al.*, 2007; Wilks, 2011). This ensures that the data from year to year are independent of each other.

The aforementioned GEV model can be viewed as a stationary process because the model parameters do not change with time so the estimated return level is a constant. Because the climate is changing, it is also reasonable to expect that the return level should change with time. By allowing the time-dependent change in the GEV parameters, the stationary model can be extended to a non-stationary model (Coles, 2001). Therefore, the statistical theory of extremes can be applied in the context of climate change. Moreover, besides examining changes in precipitation extremes with time, the non-stationary GEV model can also be used to investigate how extreme events will co-vary with external climate drivers such as the El Niño–Southern Oscillation (ENSO) phenomenon or others (Coles, 2001; Katz *et al.*, 2002; Chen and Chu, 2014; Villafuerte II *et al.*, 2015; Lu *et al.*, 2018).

It is well known that spring rainfall in Taiwan is positively correlated with the Niño3 sea surface temperature of the preceding winter (Chen *et al.*, 2003; Jiang *et al.*, 2003). During a strong El Niño event, a low-level anomalous anticyclone tends to be established over the Philippine Sea (Wang *et al.*, 2000). This Philippine Sea anticyclone induces moist southwesterly flows from the South China Sea to the north, resulting in low-level moisture convergence and heavy rainfall in Taiwan. However, by analysing the variability of spring rainfall in Taiwan from each individual event, Chen *et al.* (2008) noted that not all El Niño events lead to high spring rainfall and some may even bring below-normal spring rainfall. Changes in the position of the anomalous low-level anticyclone and the Pacific Walker circulation are postulated to be the cause of the spring wet and dry conditions in Taiwan associated with an El Niño event. It is not known whether summer rainfall in Taiwan is modulated by the antecedent El Niño event.

Tropical cyclone (TC) activity in the western North Pacific is closely related to ENSO events. Many aspects of TC's are affected by ENSO including formation location, intensity, track, lifetime, and landfall (e.g., Wang and Chan, 2000; Chu, 2004). One major source of extreme precipitation in Taiwan is caused by typhoons. A case in point was

Typhoon Morakot, which made landfall in August 2009 and killed more than 600 people. Typhoon Morakot's movement was very slow and resulted in one of the highest recorded rainfall amounts in southern Taiwan for the past 50 years (Chien and Kuo, 2011). The 3-day accumulated rainfall produced by this storm exceeded 2,000 mm at many gages.

According to the Central Weather Bureau (CWB), a total of 383 typhoons made landfall in Taiwan between 1897 and 2003. The mean annual number of typhoons that make landfall in Taiwan is about 3.58. The typhoon season in Taiwan is from July through October, where August has the highest count of typhoons, followed by July and September (Tu *et al.*, 2009). The typhoon season is the main rainy season in Taiwan. Rainfall during this period is contributed by TCs, mesoscale convective disturbances, or local thunderstorms associated with the diurnal heating patterns embedded in the prevailing southwesterly monsoon (Chen and Chen, 2003; Chen *et al.*, 2007). Chen *et al.* (2004) noted that the contribution of typhoon rainfall overwhelms that from convective systems over eastern and northern Taiwan at the height of summer. For southwestern Taiwan, which is located on the windwards side of the southwesterly flows, typhoon rainfall is comparable to that of convective rainfall. Based on a Bayesian change-point analysis, Tu *et al.* (2009) noted an abrupt increase of typhoon activity in the vicinity of Taiwan since 2000. Chu *et al.* (2014) found an increase in precipitation intensity during the typhoon season over the last 60 years in Taiwan which can be attributed to both an increase in typhoon rainfall and the monsoon rainfall. However, the data used in Tu *et al.* (2009) are seasonal typhoon counts and those in Chu *et al.* (2014) are climate change indices, not the block maximum series employed in the current study. Moreover, these two studies (Tu *et al.*, 2009; Chu *et al.*, 2014) do not use the GEV distribution.

The objective for this study is to (a) investigate the long-term trends for the 24-hr maximum precipitation as induced by typhoons during the typhoon season using data from 20 long-term stations in Taiwan; (b) investigate the spatial patterns of trends for the 2, 20, and 100-year return levels; and (c) examine the change in return levels with external climate forcing. The study is organized as follows. Sections 2 and 3 describe the data and methods used in this study, respectively. Section 4 presents the results, and the summary and discussion are in section 5.

## 2 | DATA

Long-term hourly rainfall data from 1958 to 2013 (56 years) are available from the CWB. The extreme-value data used in this study are the maximum 24-hr precipitation values during the typhoon season. Therefore, a moving window covering the true maximum 24-hr event is chosen, not precipitation accumulated for a fixed 24-hr interval in each year. Figure 1 shows the location of these 20 stations across Taiwan. The



TABLE 2 The GEV and NGEV models used in this study

Model	GEV/NGEV	Parameters		
		Location $\mu$	Scale $\sigma$	Shape $\xi$
GEV_STN	GEV ( $\mu, \sigma, \xi$ )	Constant	Constant	Constant
NGEV_TIME	NGEV ( $\mu_t, \sigma_t, \xi$ )	Time varying	Time varying	Constant
NGEV_ENSO	NGEV ( $\mu_{\text{ONI}}, \sigma_{\text{ONI}}, \xi$ )	ENSO varying	ENSO varying	Constant
NGEV_TIMEENSO	NGEV ( $\mu_t, \mu_{\text{ONI}}, \sigma_t, \sigma_{\text{ONI}}, \xi$ )	Both time and ENSO varying	Both time and ENSO varying	Constant

strong episodes. According to this definition, eight El Niño (or warm) events (1957/1958, 1965/1966, 1972/1973, 1982/1983, 1986/1987, 1991/1992, 1997/1998, 2009/2010) and eight La Niña (or cold) events (1970/1971, 1973/1974, 1975/1976, 1988/1989, 1998/1999, 1999/2000, 2007/2008, and 2010/2011) are identified during 1958–2013. For example, the 1982/1983 warm event means that ONI anomalies are used from December 1982 to February 1983.

### 3 | METHODS

#### 3.1 | Trend analysis

The trends of the precipitation extremes are estimated by the nonparametric rank-based, Mann–Kendall tests and Sen’s method under the null hypothesis of no trends. These two methods do not make any assumptions about the distribution of the data (i.e., nonparametric). The former approach tests whether the trend is monotonically increasing or decreasing. This test also estimates the significance of the trend, while the Sen’s method quantifies the slope of the trend (Mann, 1945; Sen, 1968). The slopes of all data pairs are calculated and the median of these slopes is the Sen’s estimator of slope. The advantage of these two methods is that missing observations are allowed, the data do not need to conform to any parametric distribution, and the test is robust against skewed distributions and outliers. For simplicity, these two methods are called the Mann-Kendall and Sen (MKS) test in this study. Details for these two methods can be found in Chu *et al.* (2010) and Garza *et al.* (2012).

#### 3.2 | Statistical field significance

We evaluate the significant increasing and significant decreasing trend using the MKS test based on a 10% two-sided significance level. This level implies that approximately 5% of the stations show significant increasing and significant decreasing trends by random chance. For a given data set, it is reasonable to expect a certain number of stations to pass a random local significance test. At the specified test level, 10% of all stations might be significant by chance even if the true slopes are zero. Because of the spatial correlation of the underlying geophysical data, it is also necessary to address the collective significance of a finite set of individual hypothesis tests for the entire field (Wilks, 2011; Chen and Chu, 2014).

The field significance of trends is evaluated by Monte Carlo simulations (e.g., Chu *et al.*, 2010; Westra *et al.*, 2013). The statistical inference of “field significance” is approached using the following steps. First, a matrix “ $M$ ” of the seasonal maximum daily rainfall is created with  $T$  rows and  $S$  columns, where  $T$  denotes time and  $S$  denotes spatial location of stations. Second, the rows of  $T$  are resampled 1,000 times with replacement to form new random matrices  $M_1, M_2, \dots, M_{1000}$ . By doing so, the time order in the original data is scrambled while the spatial dependence is preserved. Third, the MKS test, described in section 3.1, is then conducted to count the percentage of stations showing significant positive or negative trends separately. This procedure is then repeated for all resampled matrices. Fourth, the empirical distribution of the percentage of stations with significant trends from the random samples is established. Lastly, the observed percentage of trends is compared to those simulated by the Monte Carlo experiment. The field is considered to be significant if the observed percentage of significant positive or negative trend lies outside the central 95% region of the random statistics.

#### 3.3 | Stationary GEV distribution (GEV\_STN)

The stationary GEV distribution is often found to be a good approximation of the statistics of the maxima of long sequences of random variables. The CDF of the stationary GEV distribution is given by

$$F(z) = \exp \left\{ - \left[ 1 + \xi \left( \frac{z - \mu}{\sigma} \right) \right]^{-1/\xi} \right\}, 1 + \xi \left( \frac{z - \mu}{\sigma} \right) > 0, \quad (1)$$

where  $\mu$ ,  $\sigma$ , and  $\xi$  are the location, scale, and shape parameter, respectively. The location parameter specifies the centre of the distribution, while the scale parameter determines the size of deviations about the location parameter and the shape parameter governs how rapidly the upper tail decays (Katz, 2010). The distribution of hydrometeorological variables is often heavy tailed to the right. The introduction of a shape parameter in a GEV distribution generally improves the fit to the right tail of the distribution (i.e., extremely large values).

The GEV parameters can be fitted by maximum likelihood estimation (MLE), which maximizes the likelihood function. An alternative fitting method is the  $L$ -moments, which can be seen as a modification of the probability-weighted moments (Hosking and Wallis, 2005; Chu *et al.*,

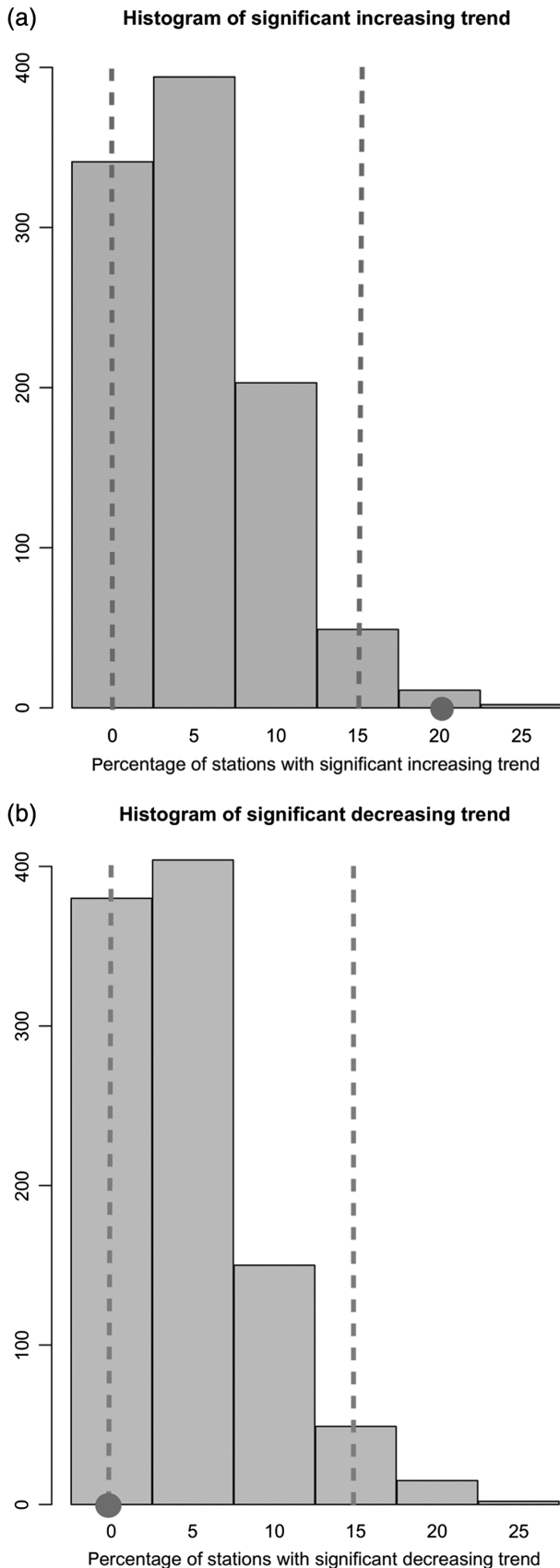


**FIGURE 2** Percentage of stations showing (a) significant positive and (b) significant negative trends for maximum 24-hr precipitation during the typhoon season (JASO) based on the Mann–Kendall and Sen’s test. The histogram is obtained from resampling with 1,000 replicates and the vertical broken lines denote the 95% of the resampled distribution. The dot is from observations

2009). *L*-moment statistics rely on ordered samples and yield robust estimates when the training sample size is small or when outliers exist (Hosking *et al.*, 1985). Because the *L*-moment method is not available to the non-stationary GEV models, the MLE is used.

Estimates of the extreme quantiles, known as the return level  $z_p$ , corresponding to the return period ( $\tau$ ),

$$\tau = 1/p, \tag{2}$$

where  $p$  is the probability of annual occurrence, can be obtained by

$$z_p = \mu - \frac{\sigma}{\xi} \left[ 1 - \{ -\log(1-p) \}^{-\xi} \right], \xi \neq 0. \tag{3}$$

The return level is expressed as the same unit as rainfall, also in millimetre, and is exceeded by the annual maximum value in any particular year with probability  $p$ . As implied in Equation (3), the behaviour of  $z_p$  depends on the location, scale, and shape parameters, and the return period  $\tau$ . The distribution will have a heavy tail when the shape parameter is greater than zero, which implies a higher probability of the presence of extreme values. That is, the probability density function decreases very slowly in the upper tail. The shape parameter is usually greater than zero for precipitation data. For convenience, the stationary GEV model is hereafter referred to as GEV\_STN.

### 3.4 | Non-stationary GEV distribution (NGEV)

Now we extend the stationary GEV model to the non-stationary one by allowing the GEV parameters to vary with time or through other climate drivers. Because the variability of the shape ( $\zeta$ ) parameter is small (Hosking *et al.*, 1985) and allowing the shape parameter to vary would likely cause numerical problems (R. Katz, personal communication, January 6, 2012), the assumptions of the two other parameters are

$$\mu_t = \mu_0 + \mu_1 t,$$

$$\log \sigma_t = \sigma_0 + \sigma_1 t, \xi \text{ is constant}, \tag{4}$$

where  $t$  stands for a time index. The exponential expression for the scale parameter  $\sigma$  is used to guarantee a positive value for  $\sigma_t$ . The coefficients  $\mu_0$  and  $\sigma_0$  are the intercept values of the NGEV parameters. The slope coefficients  $\mu_1$  and  $\sigma_1$  specify the rate of change in the parameters. Substituting Equation (4) into Equation (3), the return level  $z_p$  of a NGEV becomes

$$z_p(t) = \mu_0 + \mu_1 t - \frac{\exp[\sigma_0 + \sigma_1 t]}{\xi} \left[ 1 - \{ -\log(1-p) \}^{-\xi} \right], \xi \neq 0. \tag{5}$$

Besides the location and scale parameters and  $p$ , it is now obvious that the return level  $z_p$  is also a function of time. For  $p = 0.63$ , corresponding to return level periods greater than 1.59 year, the term

$$\frac{1}{\xi} \left[ 1 - \{ -\log(1-p) \}^{-\xi} \right]$$

is negative for any sign of the shape parameter  $\xi$  (Garcia *et al.*, 2007). Because of the negative sign in front of this term in Equation (5), it implies increasing (decreasing) return levels with time when the scale parameter  $\sigma$  is characterized by a positive (negative) slope. This term becomes more negative as  $p$  decreases. That is, the increasing (decreasing) return level with time becomes more distinct as  $p$  decreases, say, from 0.5 (2-year return period) to 0.01 (100-year return period). The same effect of this term is also realized when the time index is replaced by the ENSO index. The relative role of a positive (or negative) slope of the location and scale parameters in shaping the trend of return levels is described in details in Chen and Chu (2014).

The model shown in Equation (5), with both time-varying location and scale parameters, is referred to as NGEV\_TIME. The parameters of the non-stationary GEV distribution are estimated by the Extreme Toolkit using the R statistical programming language developed by University Corporation for Atmospheric Research (UCAR), which is available online (<http://www.isse.ucar.edu/extremevalues/evtk.html>) and in a short article (Gilleland and Katz, 2011).

In addition to estimating changes in extreme precipitation with time,  $t$  in Equation (4) can be replaced by a time-varying Niño indicator (e.g., ONI<sub>*t*</sub>). Thus, another set of location and scale parameters can be estimated to show the relationship between the precipitation extremes in Taiwan and the El Niño conditions. This third model, with both location and scale parameters dependent on the ENSO condition, is known as NGEV\_ENSO. Taking one step further, it is also of interest to include both the time index and precursory ENSO conditions in the NGEV model. For this bivariate NGEV model, the location and scale parameters are follows:

$$\begin{aligned} \mu_{t, \text{ONI}_t} &= [1, t, \text{ONI}_t] \begin{bmatrix} \mu_0 \\ \mu_1 \\ \mu_2 \end{bmatrix}, \\ \log \sigma_{t, \text{ONI}_t} &= [1, t, \text{ONI}_t] \begin{bmatrix} \sigma_0 \\ \sigma_1 \\ \sigma_2 \end{bmatrix}. \end{aligned} \quad (6)$$

The return level  $z_p$  is now governed jointly by both time index and the state of ENSO as

$$\begin{aligned} z_p(t, \text{ONI}_t) &= \mu_0 + \mu_1 t + \mu_2 \text{ONI}_t \\ &- \frac{\exp[\sigma_0 + \sigma_1 t + \sigma_2 \text{ONI}_t]}{\xi} \left[ 1 - \{-\log(1-p)\}^{-\xi} \right], \xi \neq 0. \end{aligned} \quad (7)$$

This fourth model, with both time-dependent and ENSO-dependent location and scale parameters, is referred to as NGEV\_TIMEENSO. The stationary GEV and three non-stationary GEV models are summarized in Table 2.

**Histogram of increasing trend**

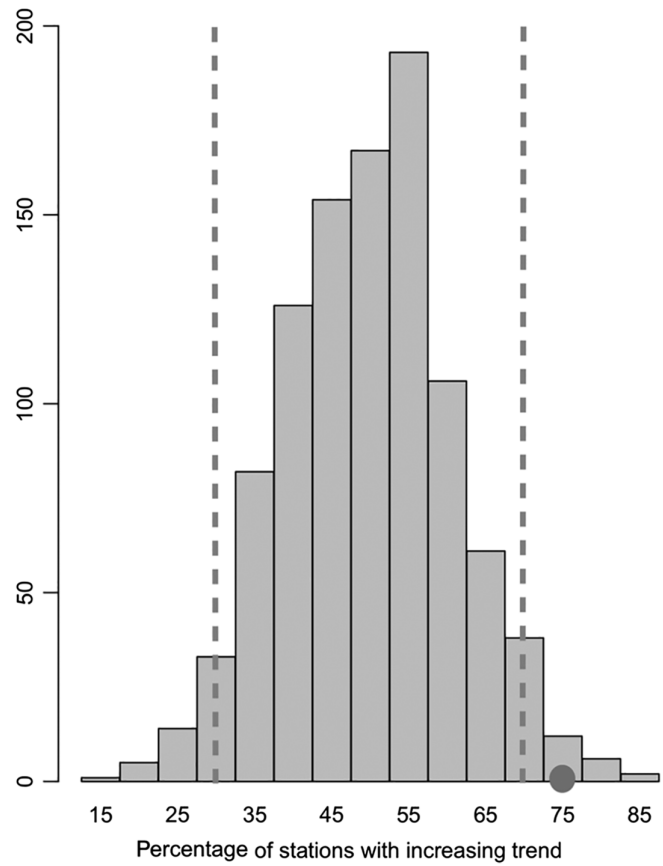


**FIGURE 3** Percentage of stations showing positive trends for maximum 24-hr precipitation during the typhoon season (JASO) based on the Mann-Kendall and Sen's test. The histogram is obtained from resampling with 1,000 replicates and the vertical lines denote the 95% of the resampled distribution. The dot is from observations

### 3.5 | Model selection

For each station, four candidate models are considered. In keeping up with the principle of parsimony, the simplest model that can explain most variations in the block maximum series should be adopted (Coles, 2001). One common way to select the best fitting model among the four is to use the Akaike information criterion (AIC). It is expressed mathematically as

$$\text{AIC} = -2L(b) + 2K, \quad (8)$$

where  $L(b)$  is the log-likelihood for a fitted model,  $b$  the parameters, and  $K$  the total number of parameters required to be estimated for each model. The first term on the right-hand side of Equation (8) represents the model performance and the second term is a penalty function for the  $K$  parameters that need to be estimated when an extreme value distribution model is fit to the data. As more parameters are brought into the model, the first term will usually decrease but the second term will necessarily increase. In general, a model with the minimum AIC value is preferred to others.

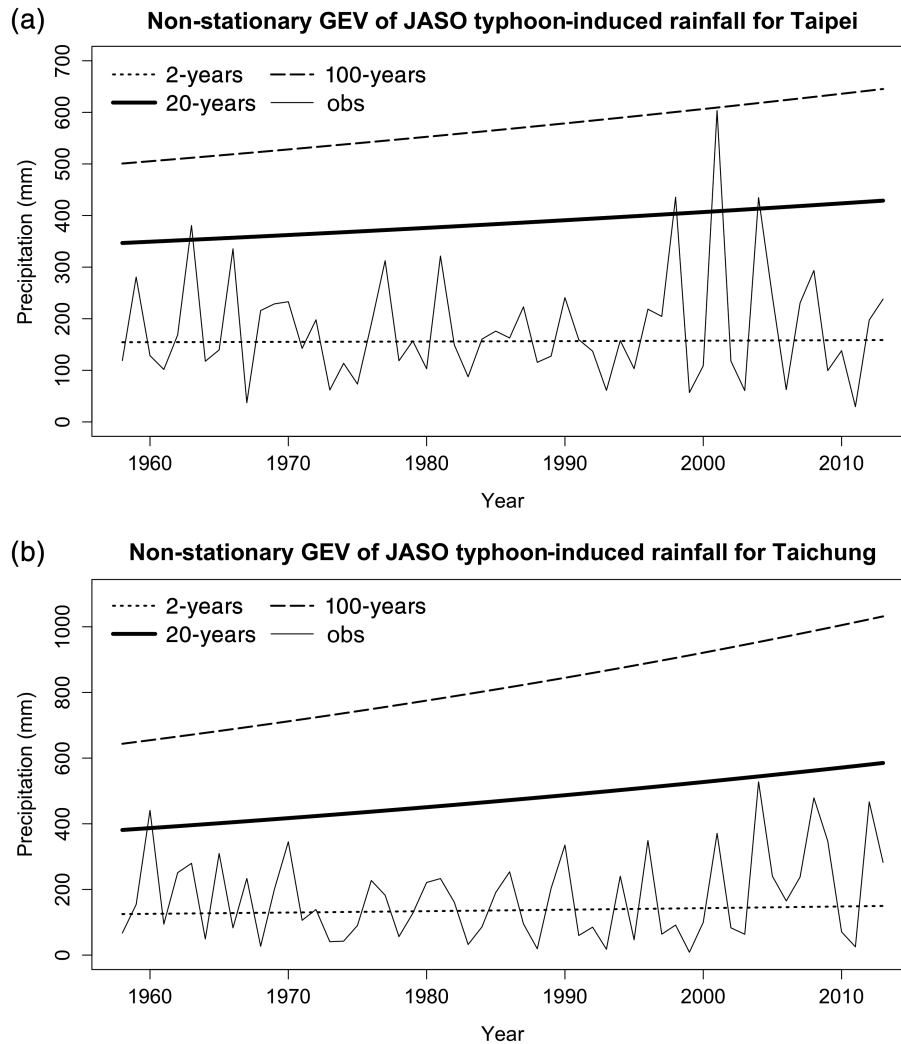


**FIGURE 4** Time series of return levels for maximum 24-hr precipitation at (a) Taipei and (b) Taichung according to the non-stationary, time-varying GEV model (NGEV\_TIME). The dotted, solid, and dashed curves denote the 2-, 20-, and 100-year return levels, respectively. Solid thin line at the bottom represents observation data

## 4 | RESULTS

### 4.1 | Trend analysis

As listed in Table 1 (fourth column), the majority of stations in Taiwan experienced an upward trend in precipitation extremes induced by typhoons since 1958. Specifically, 15 out of all 20 stations (75%) exhibit an upward trend and three of these stations are statistically significant at the 10% level of a two-sided test. This significance level implies that about 5% of stations would show significant increasing (extreme right tail) and significant decreasing (extreme left tail) trends by random chance. On the other hand, 5 out of 20 stations show a downwards trend and none of them are statistically significant. Interestingly, except for Chenggong, four stations with a downwards trend are located in northern Taiwan (Keelung, Anbu, Zhuzihu, and Taipei). In summary, long-term upwards trends in the block maximum series induced by typhoons during the typhoon season prevail in

Taiwan over the last 56 years and downward trends are found only in a few stations, mainly in northern Taiwan.

The next question is whether the significant positive trend at 3 stations out of 15 in Table 1 could have occurred by random chance. The percentage of stations with a significant positive trend falls outside the empirical distribution based on 1,000 replicates, suggesting that the observed field is significant (Figure 2a). In contrast, because no stations show significant negative trends in Table 1, the resampling test also reflects this fact (Figure 2b). That is, the field significance cannot be reached if there is not a single station exhibiting significant negative trend. Because there are increasing trends at 15 stations and such a trend is prevailing, we extend the field significance test by evaluating the distribution of the increasing trend under the null hypothesis of no trend. Again, the observed percentage of stations with a positive trend lies outside the empirical distribution (Figure 3). This result suggests that the collection of positive trends observed at three quarters of all stations during the

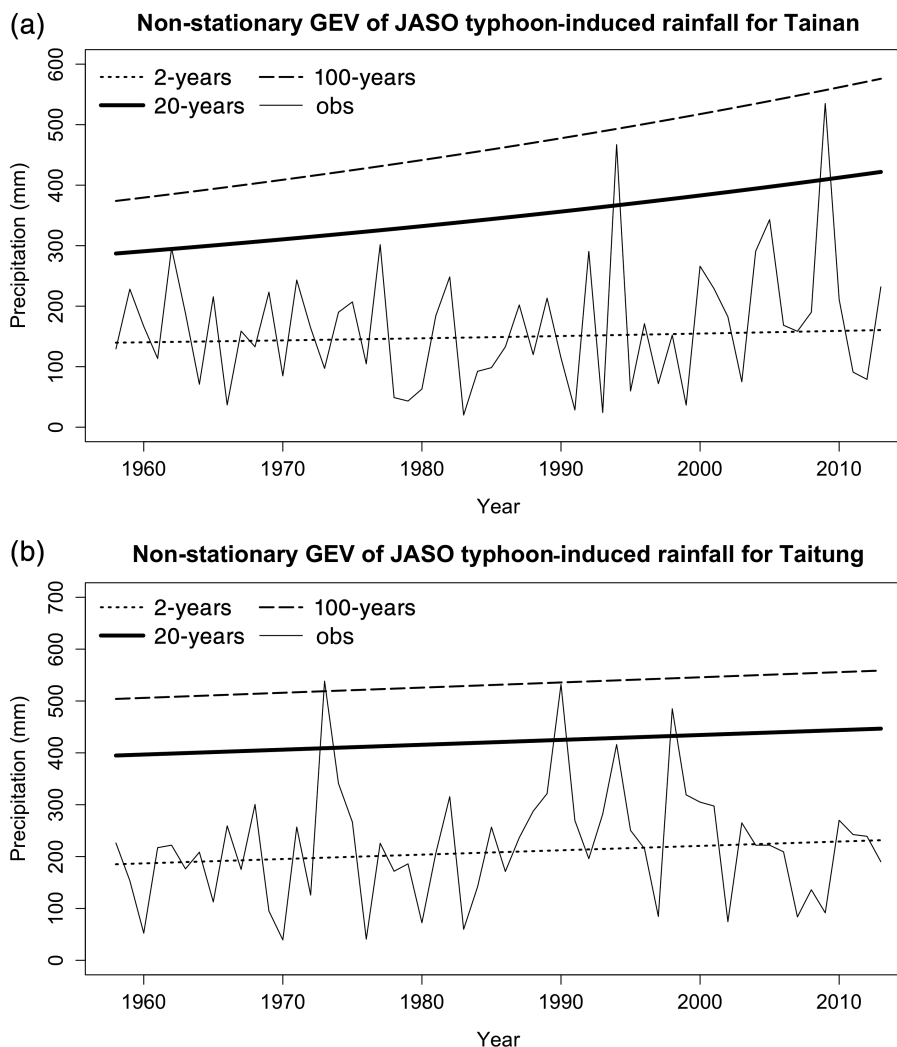


FIGURE 5 Same as Figure 4 but for (a) Tainan and (b) Taitung

typhoon season in Taiwan is quite unique and is not due to random variability.

#### 4.2 | Regional changes in return levels as a function of time (NGEV\_TIME)

Now let us turn our attention to the fifth and sixth columns in Table 1, which show the sign of the slope of the location and scale parameters, respectively, from the NGEV model with time as a covariate. As shown in Equation (5), the trend of the return level,  $z_p$ , is determined by three components—location parameter, scale parameter, and probability,  $p$ . The value of the probability is inversely related to return period, as  $\tau = 1/p$ . Note that 12 stations (60%) in Table 1 are marked by positive trend in both location and scale parameters. Seven stations see a negative trend in location but a positive trend in scale parameter. Only one station (Chenggong) is marked by a negative trend in both location and scale parameters.

In this section, we will show the time series plots of 24-hr precipitation extremes and the three return levels (2, 20, and 100 years) for six stations representative of the

region of Taiwan. The main island of Taiwan is conventionally divided into the northern, central, southern, and eastern regions. Therefore, we will adopt stations Taipei, Taichung, Tainan, and Taitung to represent these four regions, respectively. Because of the presence of the CMR which runs from the north of the island to the south with its tallest peak at Yushan (3,952 m), we also select one station, Alishan, to represent the high mountain region in central Taiwan, which is different from Taichung at a lower elevation (Table 1). For the off island stations, we chose Penghu because it has the largest population. In all, six stations are selected for the following analysis.

According to Equation (5), a positive slope of the location parameter will result in an increase in the return level and vice versa. If the scale parameter also shows a positive trend, the trend of return level  $z_p$  will increase as  $p$  decreases, which means an increase in return periods. For Taipei, a negative trend in the location parameter is embedded in a positive trend in scale parameter (Table 1). As such, the trend in return levels become more complicated. From Equation (5), a negative trend for the location parameter alone will inherently induce a negative trend for the return

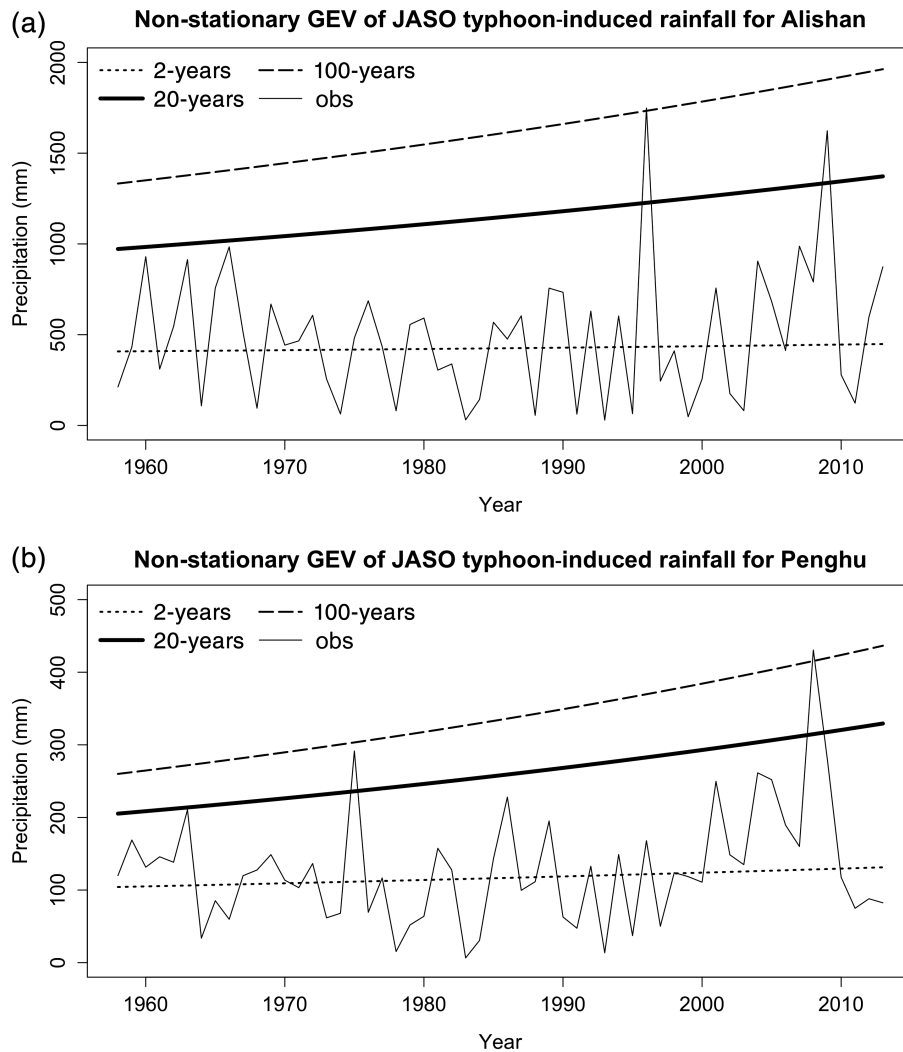


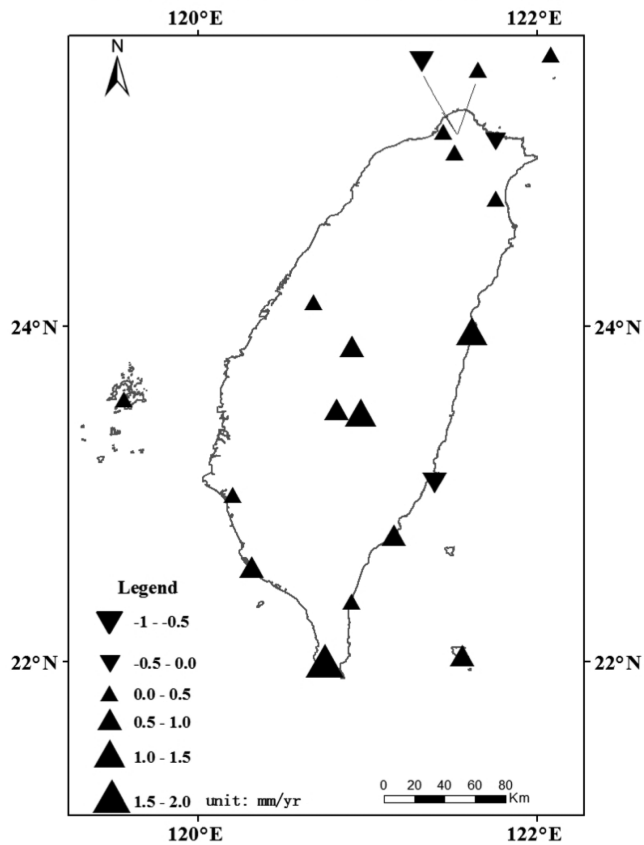
FIGURE 6 Same as Figure 4 but for (a) Alishan and (b) Penghu

level, if other components remain unchanged. However, for a positive trend in the scale parameter alone, the return levels tend to increase. Therefore, when these two opposing trends are considered jointly, there is a possibility that the trend in return levels will be gently upward such as Taipei (Figure 4a) or downward (Anbu not shown). Noted that changes in scale parameter dominate changes in location parameter for more extreme events (Katz and Brown, 1992). Therefore, for low probability (i.e., 20- or 100-year return levels), the positive trend of scale parameter overwhelms the negative trend in location parameter, yielding a positive trend in return levels.

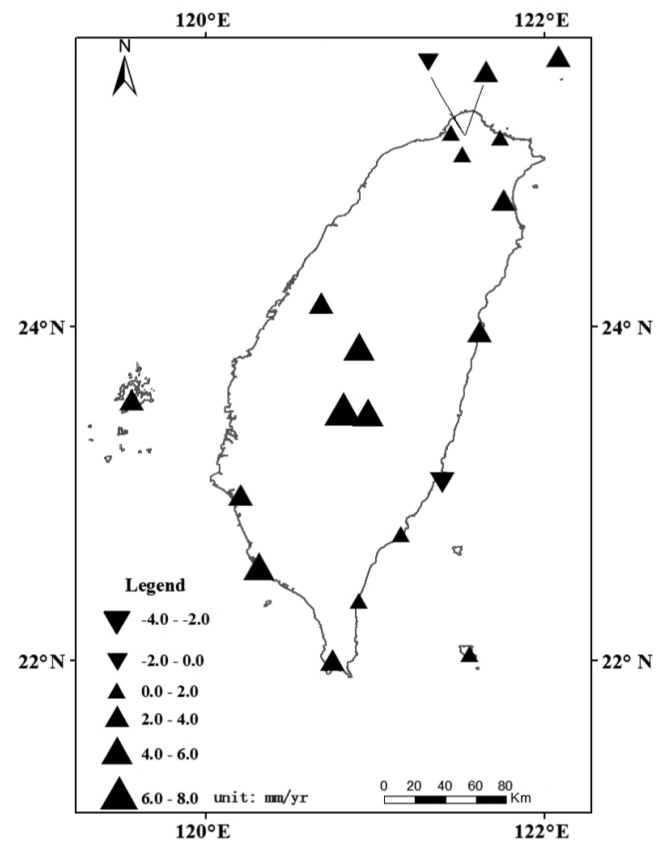
For Taichung (Figure 4b), Tainan (Figure 5a), Taitung (Figure 5b), and Penghu (Figure 6b), both the location and scale parameters exhibit a positive trend (Table 1). Therefore, the slope of return levels tends to increase with time. Take Taichung as an example. The 20-year return level was 381 mm in 1958 and increased to 585 mm by 2013. This amounts to a sizable 54% increase in 20-year return level over a span of 56 years. Another way to interpret this result is that an event with a 20-year return-interval threshold value

in 1958 occurred on average once every 13 years by 2013. Therefore, the waiting time for an extreme event that usually occurred on an average once in 20 years has shortened considerably to only once in 13 years in recent years. Also note that the slope of return levels becomes steeper as return periods increase from 2 to 100 years (as the probability of annual occurrence decreases from Equation (5)). For Alishan, the signs of these two parameters are opposite (Table 1) and a positive trend in return levels for 20 and 100 years is noted (Figure 6a). Being located in the CMR and because of topographically enhanced precipitation by typhoons, the block maximum series at Alishan show an increasing values since the mid-1990s and punctured by two extraordinarily large peaks in 1996 (1,749 mm) and 2009 (1,623 mm). The highest recorded 24-hr value in 1996 was due to Typhoon Herb, which made landfall in Taiwan on July 31. The second highest amount in 2009 was also caused by a typhoon-terrain enhancement when Morakot devastated Taiwan in August 2009. The 20-year return level at Alishan goes from nearly 972 mm in 1958 to 1,372 mm in 2013, corresponding to a considerable 41% increase in maximum

(a) Trend of non-stationary GEV return level (2-year)



(b) Trend of non-stationary GEV return level (20-year)



(c) Trend of non-stationary GEV return level (100-year)

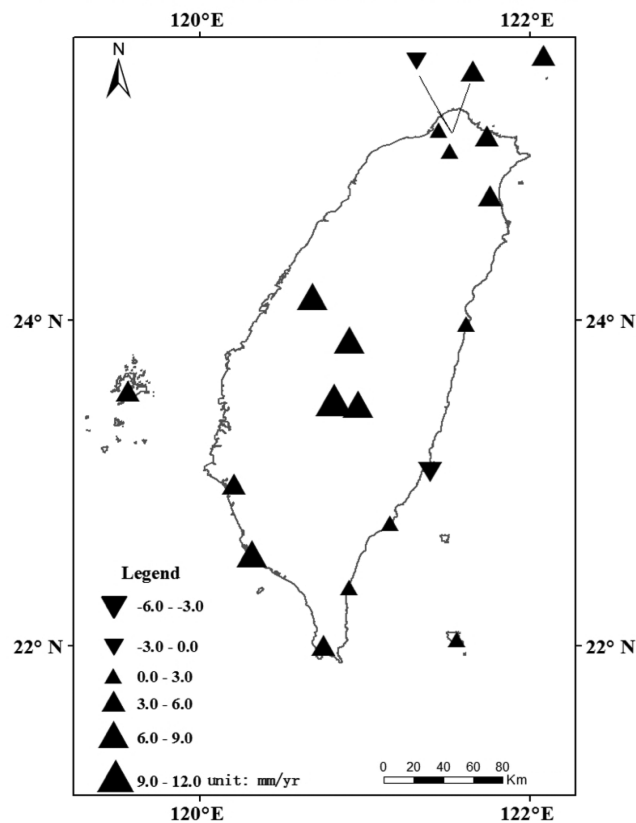


**FIGURE 7** Spatial patterns of trends for return levels from a NGEV model with time as covariate (NGEV\_TIME) for maximum 24-hr precipitation, (a) 2, (b) 20, and (c) 100 years. Triangles denote the location of the individual stations. Upwards (downwards) triangles indicate positive (negative) trend, and their size corresponds to the magnitude of the trend in the legend. Note that all stations are significant at the 5% level

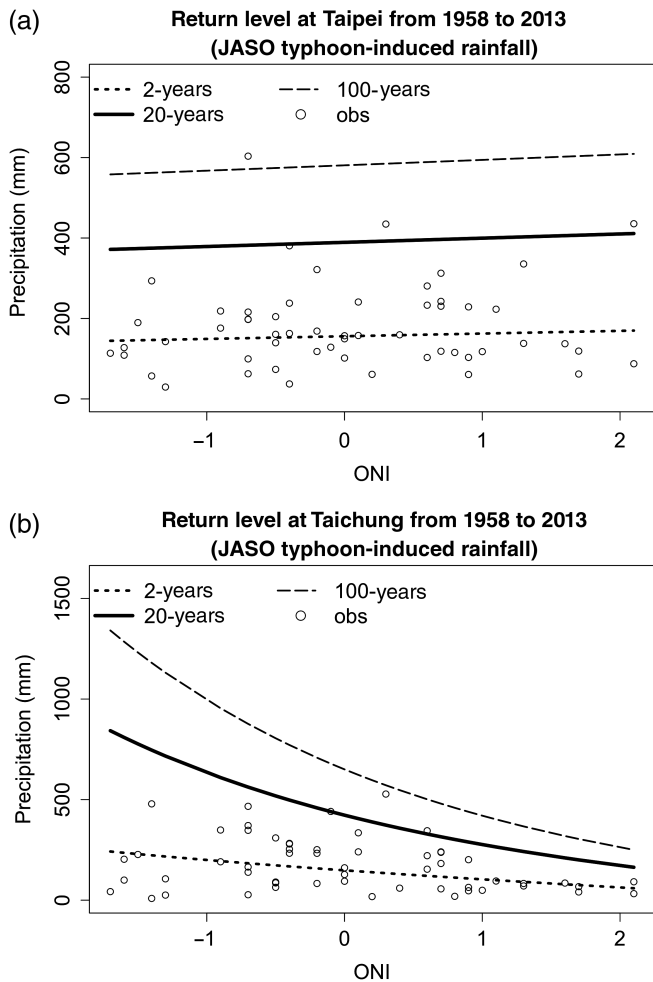


**FIGURE 8** Relationship between return levels of maximum 24-hr precipitation and ONI at (a) Taipei and (b) Taichung according to the non-stationary, ENSO-varying GEV model (NGEV\_ENSO). The short dashed, solid, and dashed curves denote the 2-, 20-, and 100-year return levels, respectively. Open circles denote observation data

24-hr rainfall over the last 56 years. One of the stations with the lowest recorded 24-hr maximum rainfall (6.5 mm in 1983) is Penghu, which is located on the offshore island west of Taiwan (Figures 1 and 6b). Even though Penghu is very dry, the return levels of 20 and 100 years still exhibit an increasing trend over time, and the percentage of increase from 1958 to 2013 is substantial (Figure 6b).

The spatial patterns of the trends in the three return levels of the 24-hr maximum precipitation during the typhoon season for the NGEV with time as a covariate for all 20 stations are found in Figure 7. The return periods (2, 20, and 100 years) in Figure 7 represent the annual probabilities of 0.5, 0.05, and 0.01, respectively. Figure 7a shows that a large majority of the stations, denoted by triangles pointing upwards, have a positive slope in 2-year return level except for three stations. Figure 7b,c shows that the 20- and 100-year return levels for all stations are positive except for two stations (Anbu and Chenggong) which are characterized by a downward trend. Trends at all stations are significant at the 5% level. As expected, the slope of the 100-year

return level is larger than the corresponding 20- and 2-year value. In short, an increase in return levels is observed for all three return periods at a majority of stations in Taiwan over the last 56 years and this increase in rainfall extremes is associated with typhoon-induced activity. Tables for 20-yr (S1), 50-yr (S2) and 100-yr (S3) return levels for each station are listed in the Supporting Information section.

### 4.3 | Changes in return levels as a covariate of the ENSO phenomenon (NGEV\_ENSO)

The NGEV model was fitted with the ONI of the preceding winter (DJF) as a covariate. The winter index is chosen because ENSO events usually reach their peak in the boreal winter. Because the ONI changes from winter to winter and this change is not monotonically increasing or decreasing as in time, the return level values are arranged according to ONI values, not according to years. The influence of the winter ONI on precipitation extremes in the following typhoon season across Taiwan is not uniform. For example, 13 stations experience a positive influence while 7 stations show a negative relationship. For the positive influence, it means that a large and positive ONI, corresponding to an El Niño event, would favour extremely high rainfall. By the

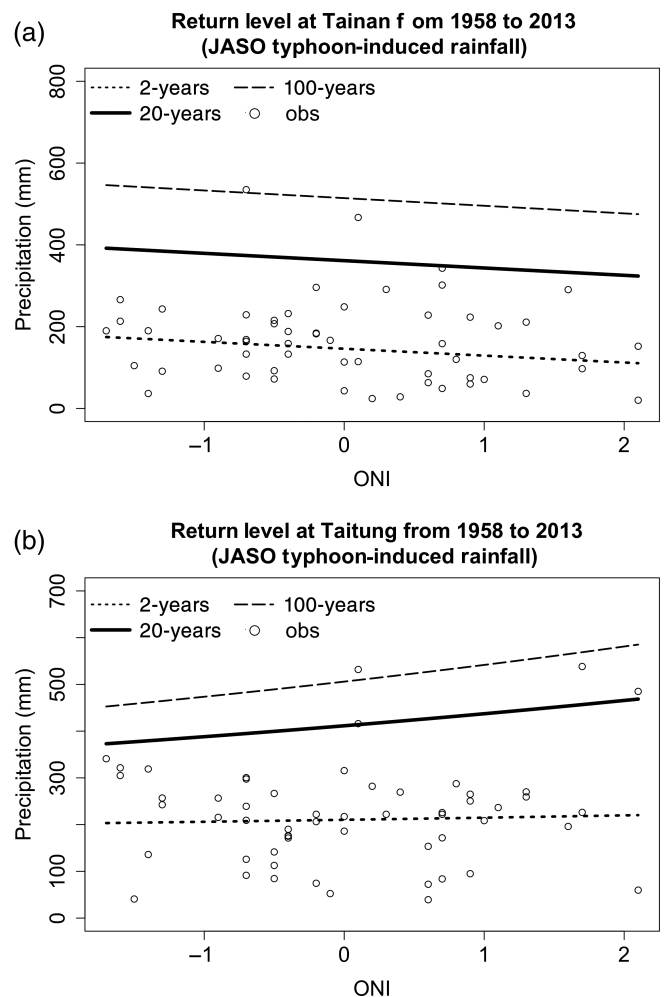


**FIGURE 9** Same as Figure 8 but for (a) Tainan and (b) Taitung

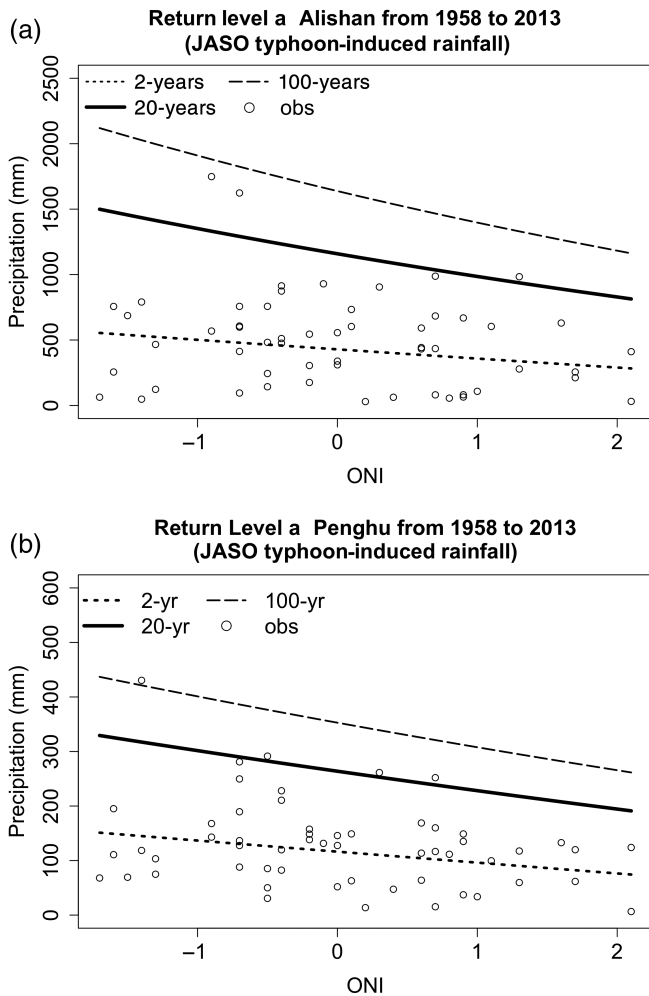


FIGURE 10 Same as Figure 8 but for (a) Alishan and (b) Penghu

same token, a large and negative ONI, corresponding to a La Niña event, results in extremely low rainfall. For stations under the positive influence of ONI, the representative stations include Taipei (Figure 8a) and Taitung (Figure 9b). For stations that show a negative relationship with ONI, the representative stations are Taichung (Figure 8b), Tainan (Figure 9a), Alishan (Figure 10a), and Penghu (Figure 10b). Based only on a time-varying location parameter, Villafuerte II *et al.* (2015) studied changes in extreme rainfall (i.e., annual maximum daily rainfall) in the Philippines and linked such changes to ENSO and global mean temperature separately. They also noted a non-uniform response of ENSO on extreme rainfall in Philippines, with a positive association in northern Philippines and a negative association in central Philippines.

To quantify the effect of ENSO on rainfall extremes, the difference in the 20-year return level between El Niño and La Niña events is divided by La Niña events (i.e.,  $[RL_{Niño} - RL_{Niña}] / RL_{Niña}$ ; Figure 11). An east-west contrast is seen in the spatial distribution of return level difference across Taiwan depending on the state of the preceding winter ENSO conditions. Stations in northern and eastern Taiwan exhibit an increasing percentage, ranging from 10 to 50%, in

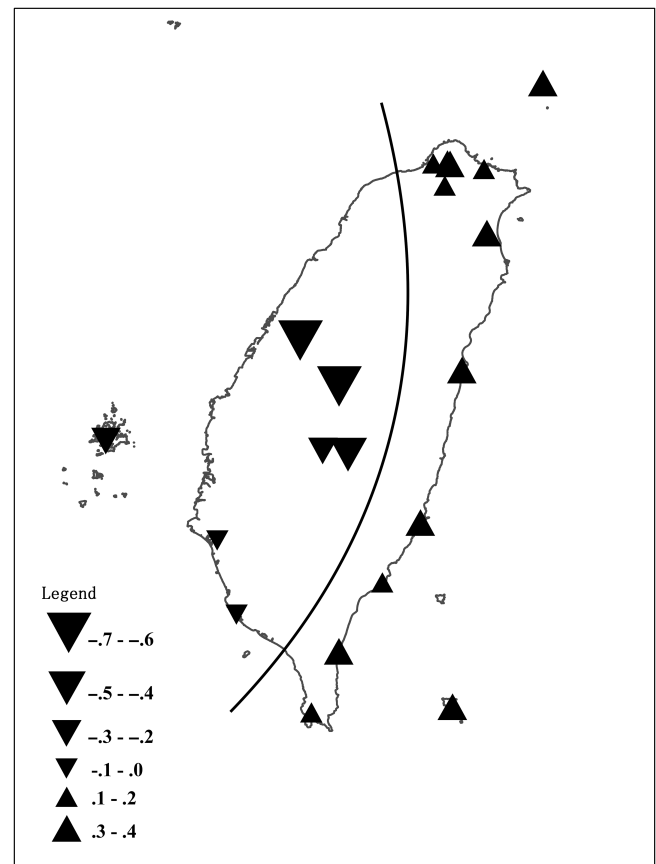


FIGURE 11 Spatial pattern of percentage difference of 20-year return levels (RL20) during the typhoon season between El Niño and La Niña events divided by La Niña events ( $[RL_{20El Niño} - RL_{20La Niña}] / RL_{20La Niña}$ ). Note that the season refers to the second year of an El Niño (La Niña) episode. Upward triangles denote higher rainfall extremes following an El Niño event and downward triangles denote lower rainfall extremes following an El Niño event

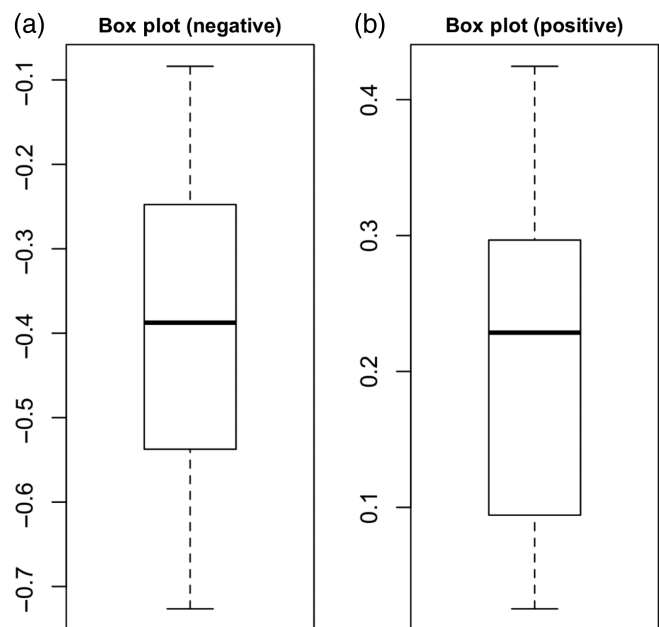
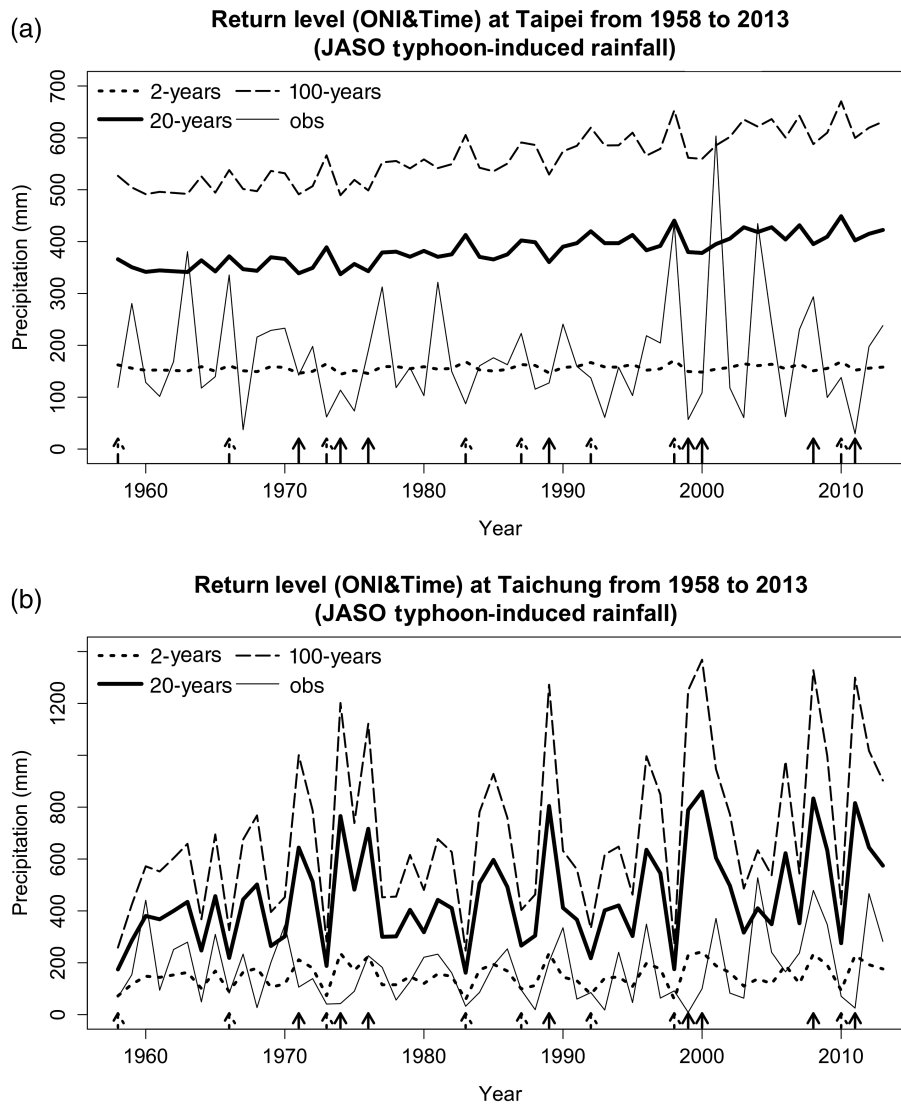


FIGURE 12 Box plots of (a) negative percentage difference and (b) positive percentage difference of 20-year return level (RL20) during the typhoon season between El Niño and La Niña events divided by La Niña events ( $[RL_{20El Niño} - RL_{20La Niña}] / RL_{20La Niña}$ ). Note that the season refers to the second year of an El Niño (La Niña) episode



**FIGURE 13** Time series of return levels for maximum 24-hr precipitation at (a) Taipei and (b) Taichung according to the non-stationary, bi-covariate GEV model (NGEV\_TIMEENSO). The short dashed, solid, and dashed curves denote the 2-, 20-, and 100-year return levels, respectively. Thin solid line at the bottom denotes observations. Solid (broken) arrows along the abscissa indicate the second year of a La Niña (El Niño) episode

return levels in JASO after an El Niño occurred, relative to a La Niña event. In the meantime, a decrease in rainfall extremes is even more pronounced by as much as 60–70% in western-central Taiwan. For stations in northern and eastern Taiwan, the median of the 20-year return level difference between El Niño and La Niña events is 23%, while the median for western-central Taiwan is –39%. In other words, an El Niño event tends to favour extremely high rainfall in the following typhoon season in northern and eastern Taiwan and extremely low rainfall in western Taiwan, including the CMR. Results for the 100-year return levels between two climate extremes are similar to that shown in Figure 11.

Figure 12 presents the boxplot, also known as the box-and-whisker plot, of the percentage changes in 20-year return level between two climate extremes for (a) western Taiwan and (b) northern/eastern Taiwan. Variability in return levels for stations in western Taiwan is greater than for stations in northern and eastern Taiwan. The location of

the median in Figure 12b (northern and eastern Taiwan) is closer to the upper end of the box, suggesting a tendency towards negative skewness. This is also consistent with the inequality of the two whisker lengths. For western Taiwan (Figure 12a), the difference in return levels between two climate extremes appears to be reasonably symmetrical as the median is located near the centre of the box and two whiskers are approximately of equal length.

#### 4.4 | Changes in return levels driven by both time and ENSO (NGEV\_TIMEENSO)

The previous two subsections focused on the changes in return levels when either time or ENSO was used as a covariate. Now we extend the NGEV analysis by considering both time and ONI as covariates and show changes in return levels as a function of time. By doing this, we can see how high-frequency inter-annual variability is embedded within

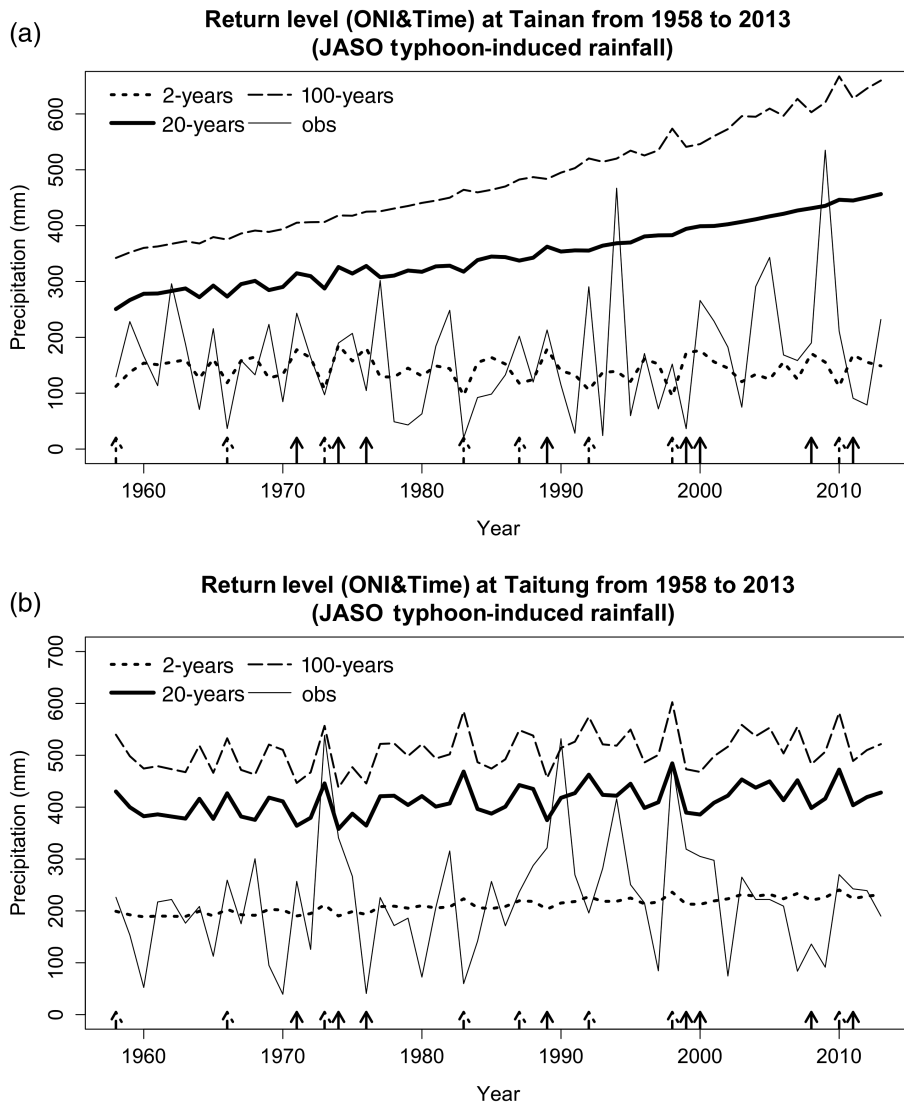


FIGURE 14 Same as Figure 13 but for (a) Tainan and (b) Taitung

the low-frequency long-term slower variations in return levels. Figure 13a displays the changes in three return levels in Taipei from 1958 to 2013. Take the 20-year return level from the bi-covariate model as an example. Instead of a rather smooth and rising line as seen in Figure 4a, the return level fluctuates at an inter-annual timescale confounded by a slow-varying long-term rising trend in Figure 13a. These features are also seen for Tainan (Figure 14a), particularly prior to 1980. The high-frequency inter-annual variations in return levels are more distinguished for Taichung (Figure 13b), Alishan (Figure 15a), and Penghu (Figure 15b). They are exemplified by the high return levels in the second year of a La Niña event (e.g., 2000 and 2008) and low return levels in the second year of an El Niño event (e.g., 1998 and 2010). They are consistent with the difference in percentage map between El Niño and La Niña events as seen in Figure 11. The results presented in Figures 13–15 suggest that the short-term inter-annual variations influenced by ENSO are more dominant than long-term time trend in return levels for

Taichung, Alishan, and Penghu. For Taitung (Figure 14b), relatively higher return level occurs in the second year of an El Niño event (e.g., 1998 and 2010).

#### 4.5 | Model selection results and uncertainty estimates

The AIC values for four candidate models in Table 2 at each individual station are tallied. Seven stations with a non-stationary model are identified to be the best fitting model while the other 13 stations indicate stationary characteristics (Figure 16). Out of these seven stations with non-stationary features, one station is identified as NGEV\_TIME (Keelung), three stations as NGEV\_ENSO (Penghu, Taichung, and Riyuetan), and three stations as NGEV\_TMEENSO (Hualien, Tainan, and Yushan). The ratio of stations with NGEV models to the total number of stations entertained is approximately one third (7/20), similar to what is found in Philippines (Villafuerte II *et al.*, 2015) and in the Yangtze River basin of China (Lu *et al.*, 2018). One cautionary note is that the difference in AIC values among four

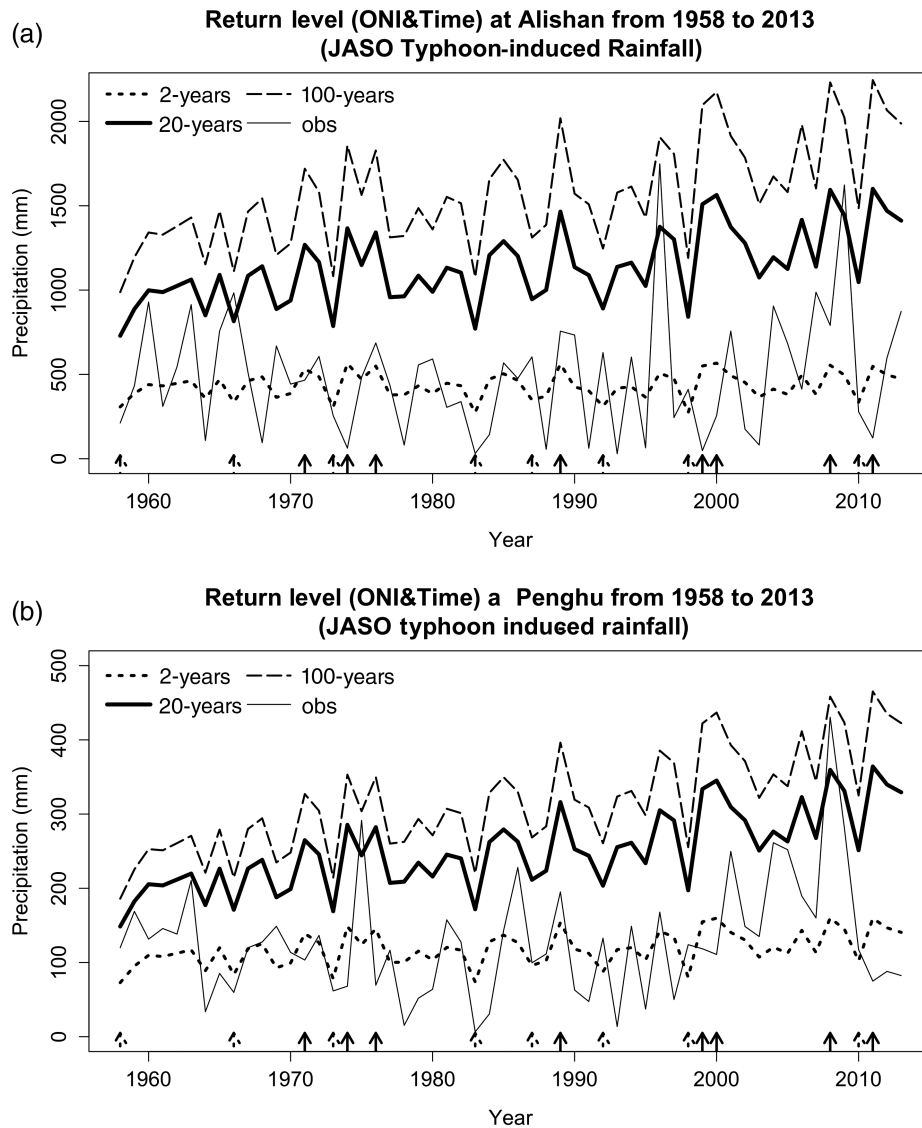


FIGURE 15 Same as Figure 13 but for (a) Alishan and (b) Penghu

candidate models for each station is rather small. On average, the ratio of the difference from the minimum to the maximum AIC values divided by the mean values among the four models is only 0.7%. Therefore, the candidate stationary and a variety of non-stationary GEV models considered are almost equally likely to be the “best” fitting model for each station and the minimum AIC criterion should not be rigidly followed.

It is also interesting to provide uncertainty estimates of return levels for all stations. Here we choose the 20- and 100-year return levels based on the bi-covariate model and use the 95% confidence interval (CI) in 2013 as uncertainty estimates (Figures 17 and 18). For a majority of stations along the east coast and southernmost tip of Taiwan as well as Penghu, the 95% CI of these two return levels is relatively low, implying lower uncertainty in estimating the return levels. The 95% CI is wider for Riyuetan, Alisan, Taichung, Kaohsiung, and Ilan. Therefore, the uncertainty for the

return levels is relatively large for those stations in which the background return level is high (Figures 13b and 15a).

### 5 | SUMMARY

Climate information about heavy rainfall events, including their frequency, intensity, and trends, is useful for decision makers in many fields. For this information to be useful, an analysis of climate risks, which involves extreme weather events and return periods, is applied. The return period statistics are commonly used for urban and highway drainage design, for potential flood risks within a watershed, and for environmental regulation. Historically, these statistics are time-invariant. Because the climate is changing, the conventional wisdom of fixed return levels used in various engineering design is questionable and should be revised by taking climate change into account. With this goal in mind, a novel non-stationary GEV model is applied to investigate

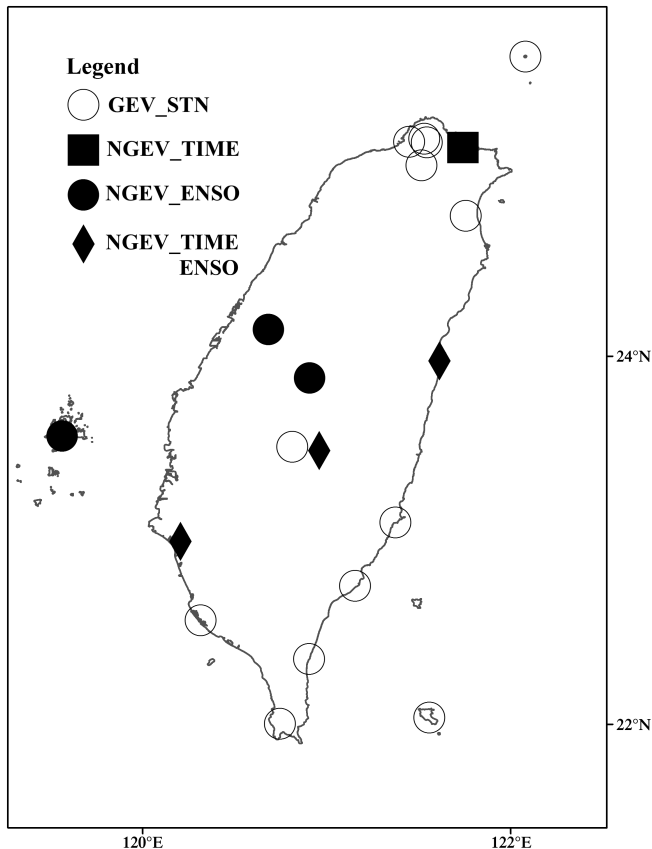


**FIGURE 16** The best fitting model for the typhoon producing seasonal maximum 24-hr precipitation according to the AIC criterion. The description for four candidate models is provided in Table 2

how (a) return levels will change in time during the typhoon season in Taiwan, and (b) how return levels will be influenced by a climate driver such as ENSO events.

The MKS trend analysis on the 24-hr precipitation extremes shows that 15 out of 20 stations have a positive trend, which implies that there is a prevailing increasing trend in precipitation extremes from 1958 to 2013 in Taiwan. The percentage of positive trends is predominant and could not have occurred by random chance based on a field significant test. This result is consistent with Chu *et al.* (2014) who used a different data set and method to demonstrate a prevailing upward trend in rainfall intensity during the typhoon season since 1950.

The extreme precipitation data were then fitted with the NGEV model where the location and scale parameters are allowed to vary with time while the shape parameter is held constant. The 20- and 100-year return level results from the NGEV model with time show that 18 stations have a positive trend, and only two stations have a negative trend (Figure 7b,c). This means that an increasing trend in return levels associated with heavy precipitation events induced by typhoons is prevalent. Therefore, more intense typhoon producing seasonal maximum 24-hr precipitation has been observed in Taiwan since 1958. Alternatively, the return-interval threshold values have shortened considerably throughout the last 56 years. That is, the frequency of

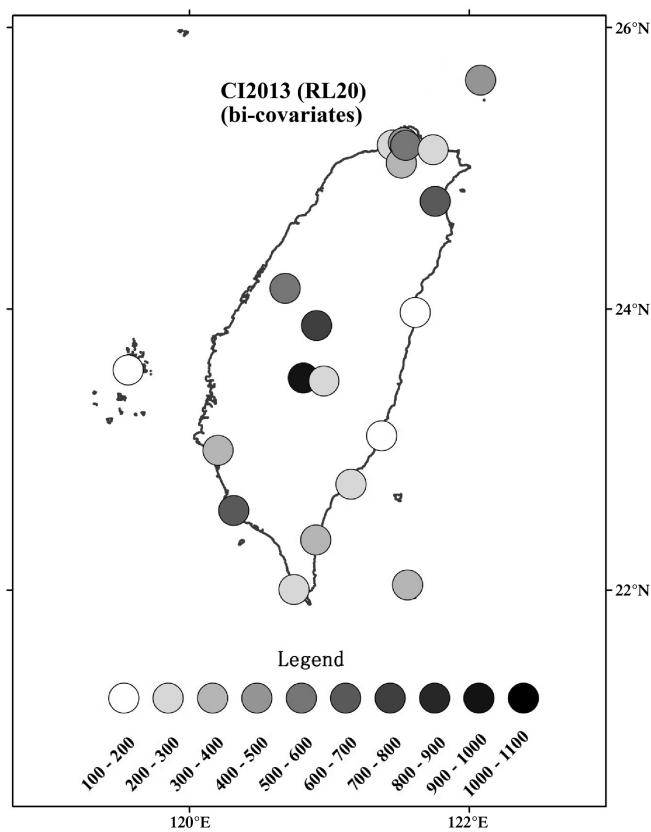


**FIGURE 17** The 95% CI (mm) for 20-year return level in 2013 based on a bi-covariate NGEV model (NGEV\_TIMEENSO)

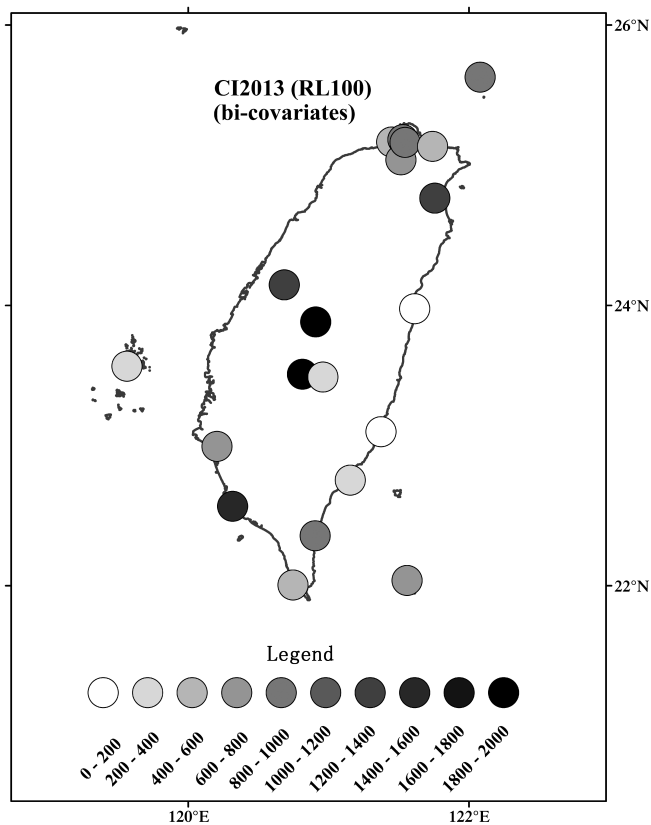


**FIGURE 18** The 95% CI (mm) for 100-year return level in 2013 based on a bi-covariate NGEV model (NGEV\_TIMEENSO)

typhoon-induced extreme precipitation has occurred more often in recent years.

Independently, the extreme precipitation data were also fitted with ONI as a covariate. The return level plots show 13 stations with a positive relationship with the preceding winter ONI and seven stations with a negative relationship with the same index. Specifically, the El Niño event favours extremely high rainfall in northern and eastern coastal Taiwan in the following typhoon season. For the 20-year return level, the increase varies from 10 to 50% during a warm event relative to a cold event. In the meantime, western Taiwan and the CMR may experience extremely low rainfall during the typhoon season following an El Niño episode. This decrease in return level of rainfall extremes in western Taiwan is more pronounced than the corresponding increase seen in northern and eastern Taiwan. Conversely, a La Niña event may result in extremely high rainfall for western Taiwan and the CMR. Therefore, an east–west regional contrast in extreme rainfall depending on state of ENSO is expected across Taiwan.

A NGEV model based on both time and ENSO as covariates is also applied in this study and changes in return levels are presented as a function of time. For most stations in the western Taiwan including the CMR and Penghu, changes in return levels are very sensitive to the ENSO phenomenon and less so to the slowly varying time trend. Specifically, higher (lower) return levels are observed in the second year of a La Niña (El Niño) event for the aforementioned areas. The results presented here may benefit many water related agencies in Taiwan (e.g., Soil and Water Conservation Bureau, Directorate General of Highways) who are concerned with recurrent flooding and the relevant policy making. Information from this study may provide important guidance to those agencies about changing characteristics of return levels so that proper hydrologic planning and management can ensue.

#### ACKNOWLEDGEMENTS

This work was funded by the Central Weather Bureau (CWB) of the Republic of China. HLC is supported by the Ministry of Science and Technology, Republic of China, under Grants MOST-104-2625-M-052-004, MOST-105-2625-M-052-001 and MOST-106-2625-M-052-001. We would like to acknowledge the keen interest and kind support from Ms. Yun-Lan Chen and Mr. Lee-Yin Shen of the CWB. The data are quality-controlled by the Manysplendid Infotech in Taiwan, and we thank Dr. Chih-Yung Feng for his contribution. Constructive comments from two anonymous reviewers helped to greatly improve the presentation of this paper. Thanks also go to May Izumi for editing the manuscript and Boyi Lu for assisting some plots.

#### ORCID

Pao-Shin Chu  <https://orcid.org/0000-0002-8425-9559>

#### REFERENCES

- Chen, C.S. and Chen, Y.-L. (2003) The rainfall characteristics of Taiwan. *Monthly Weather Review*, 131, 1323–1341.
- Chen, Y.R. and Chu, P.-S. (2014) Trends in precipitation extremes and return levels in the Hawaiian Islands under a changing climate. *International Journal of Climatology*, 34, 3913–3925.
- Chen, C.S., Chen, W.-C. and Tao, W.-K. (2004) Characteristics of heavy summer rainfall in southwestern Taiwan in relation to orographic effects. *Journal of the Meteorological Society of Japan*, 82, 1521–1543.
- Chen, G.T.J., Jiang, Z. and Wu, M.C. (2003) Spring heavy rainfall events in Taiwan during warm episodes and the associated large-scale conditions. *Monthly Weather Review*, 131, 1173–1188.
- Chen, C.S., Chen, Y.-L., Chen, W.-C. and Lin, P.-L. (2007) Statistics of rainfall occurrences in Taiwan. *Weather and Forecasting*, 22, 981–1002.
- Chen, J.M., Li, T. and Shih, C.F. (2008) Asymmetry of the El Niño–spring rainfall relationship in Taiwan. *Journal of the Meteorological Society of Japan*, 86, 297–312.
- Chien, F.C. and Kuo, H.C. (2011) On the extreme rainfall of Typhoon Morakot (2009). *Journal of Geophysical Research: Atmospheres*, 116(D5), D05104. <https://doi.org/10.1029/2010JD015092>.
- Chu, P.-S. (2004) ENSO and tropical cyclone activity. In: Murnane, R.J. and Liu, K.-B. (Eds.) *Hurricanes and Typhoons: Past, Present, and Future*. New York: Columbia University Press, pp. 297–332.
- Chu, P.-S., Zhao, X., Ruan, Y. and Grubbs, M. (2009) Extreme rainfall events in the Hawaiian Islands. *Journal of Applied Meteorology and Climatology*, 48, 502–516.
- Chu, P.-S., Chen, Y.R. and Schroeder, T.A. (2010) Changes in precipitation extremes in the Hawaiian Islands in a warming climate. *Journal of Climate*, 23, 4881–4900.
- Chu, P.-S., Chen, D.J. and Lin, P.L. (2014) Trends in precipitation extremes during the typhoon season in Taiwan over the last 60 years. *Atmospheric Science Letters*, 15(1), 37–43.
- Coles, S. (2001) *An Introduction to Statistical Modeling of Extreme Values*. London: Springer, 208 pp.
- García, J.A., Gallego, M.C., Serrano, A. and Vaquero, J.M. (2007) Trends in block-seasonal extreme rainfall over the Iberian Peninsula in the second half of the twentieth century. *Journal of Climate*, 20, 113–130.
- Garza, J., Chu, P.-S., Norton, C. and Schroeder, T.A. (2012) Changes of the prevailing trade winds over the islands of Hawaii and the North Pacific. *Journal of Geophysical Research: Atmospheres*, 117, D11109.
- Gilleland, E. and Katz, R.W. (2011) New software to analyze how extremes change over time. *Eos, Transactions American Geophysical Union*, 92(2), 13–14.
- Hosking, J.R.M. and Wallis, J.R. (2005) *Regional Frequency Analysis: An Approach Based on L-Moments*. Cambridge: Cambridge University Press, 224 pp.
- Hosking, J.R.M., Wallis, J.R. and Wood, E.F. (1985) Estimation of the generalized extreme value distribution by the method of probability-weighted moments. *Technometrics*, 27(3), 251–261.
- Jiang, Z., Chen, G.T.J. and Wu, M.-C. (2003) Large-scale circulation patterns associated with heavy spring rain events over Taiwan in strong and non-ENSO years. *Monthly Weather Review*, 131, 1769–1782.
- Katz, R.W. (2010) Statistics of extremes in climate change. *Climatic Change*, 100, 71–76.
- Katz, R.W. and Brown, B.G. (1992) Extreme events in a changing climate: variability is more important than averages. *Climatic Change*, 21, 289–302.
- Katz, R.W., Parlange, M.B. and Naveau, P. (2002) Statistics of extremes in hydrology. *Advances in Water Resources*, 25(8), 1287–1304.
- Kharin, V.V. and Zwiers, F.W. (2005) Estimating extremes in transient climate change simulations. *Journal of Climate*, 18, 1156–1173.
- Lu, M., Wu, S.-J., Chen, J., Chen, C., Wen, Z. and Huang, Y. (2018) Changes in extreme precipitation in the Yangtze River basin and its association with global mean temperature and ENSO. *International Journal of Climatology*, 38, 1989–2005.
- Mann, H.B. (1945) Nonparametric tests against trend. *Econometrica*, 13, 245–259.
- Sen, P.K. (1968) Estimates of the regression coefficient based on Kendall's tau. *Journal of the American Statistical Association*, 63(324), 1379–1389.
- Tu, J.Y., Chou, C. and Chu, P.-S. (2009) The abrupt shift of typhoon frequency in the vicinity of Taiwan and its association with western North Pacific–East Asian climate change. *Journal of Climate*, 22, 3617–3628.

- Villafuerte, M.Q., II, Matsumoto, J. and Kubota, H. (2015) Changes in extreme rainfall in the Philippines (1911–2010) linked to global mean temperature and ENSO. *International Journal of Climatology*, 35, 2033–2044.
- Wang, B. and Chan, J.C.L. (2000) How strong ENSO events affect tropical storm activity over the western North Pacific. *Journal of Climate*, 15, 1643–1658.
- Wang, B., Wu, R. and Fu, X. (2000) Pacific–East Asian teleconnection: How does ENSO affect East Asian climate? *Journal of Climate*, 13, 1517–1536.
- Westra, S., Alexander, L.V. and Zwiers, F.W. (2013) Global increasing trends in annual maximum daily precipitation. *Journal of Climate*, 26, 3904–3918.
- Wilks, D.S. (2011) *Statistical Methods in the Atmospheric Sciences*. Oxford: Academic Press, 676 pp.
- Zwiers, F.W. and Kharin, V.V. (1998) Changes in the extremes of the climate simulated by CCC GCM2 under CO<sub>2</sub> doubling. *Journal of Climate*, 11, 2200–2222.

## SUPPORTING INFORMATION

Additional supporting information may be found online in the Supporting Information section at the end of the article.

**How to cite this article:** Chu P-S, Zhang H, Chang H-L, Chen T-L, Tofte K. Trends in return levels of 24-hr precipitation extremes during the typhoon season in Taiwan. *Int J Climatol*. 2018;38: 5107–5124. <https://doi.org/10.1002/joc.5715>